Temperature Effect on the Radioluminescence of Cu-, Ce-, and CuCe-Doped Silica-Based Fiber Materials

Nourdine Kerboub, Diego Di Francesca, Sylvain Girard, Adriana Morana, Hicham El Hamzaoui, Youcef Ouerdane, Geraud Bouwmans, Remi Habert, Aziz Boukenter, Bruno Capoen, et al.

Temperature Effect on the Radioluminescence of Cu, Ce and CuCe Doped Silica-based Fiber Materials

Journal:	*IEEE Transactions on Nuclear Science*
Manuscript ID	Draft
Manuscript Type:	RADECS 2020
Date Submitted by the Author:	n/a
Complete List of Authors:	Kerboub, Nourdine; European Organization for Nuclear Research, EN Di Francesca, Diego; European Organization for Nuclear Research, ; Laboratoire Hubert Curien, GIRARD, Sylvain; CEA, DIF Morana, Adriana; Université de Lyon, Laboratoire Hubert Curien El Hamzaoui, Hicham; Université de Lille, Laboratoire PhLAM OUERDANE, Youcef; Université Saint-Etienne, UMR-CNRS 5516 Bouwmans, Geraud; Université de Lille Habert, Rémi; Université de Lille Boukenter, Aziz; Université Jean Monnet, Laboratoire H. Curien Capoen, Bruno; Université de Lille, PhLAM, UMR 8523 Marin, Emmanuel; Université de Saint-etienne, Physique Bouazaoui, Mohamed; Université de Lille, PhLAM, UMR 8523 Kadi, Yacine; CERN, Engineering; Sungkyunkwan University, Energy Science Ricci, Daniel; Istituto Nazionale di Fisica Nucleare, Perugia Alia, Ruben; CERN, Engineering Department Mekki, Julien; CNES, Brugger, Markus; CERN, EN/STI
Standard Key Words:	Radioluminescence, Optical fibers, Dosimetry, Accelerators, Space applications, Radiations, X-rays, Gamma, Silica Glass, Cerium, Copper

Temperature Effect on the Radioluminescence of Cu, Ce and CuCe Doped Silica-based Fiber Materials

Nourdine Kerboub, Diego Di Francesca, Sylvain Girard, *Senior Member, IEEE*; Adriana Morana, *Member, IEEE*, Hicham El Hamzaoui, Youcef Ouerdane, Géraud Bouwmans, Rémi Habert, Aziz Boukenter, Bruno Capoen, Emmanuel Marin, Mohamed Bouazaoui, Yacine Kadi, Daniel Ricci, Ruben Garcia Alia, Julien Mekki, Markus Brugger.

***Abstract*— We evaluate the temperature effect on the X-ray Radiation Induced Luminescence (RIL) of Cu or Ce-single-doped, and CuCe co-doped silica glass. Previous investigations showed that these optical materials exhibit interesting dosimetry properties, such as very good detection capabilities and linear response over a large range of dose rate. However, several radiation environments, such as space and particle accelerators, require also a careful assessment of the temperature effect. With this aim, we characterize their RIL efficiency and spectral dependence at several irradiation temperatures. We demonstrate that all the investigated materials present a non-negligible temperature dependence of the RIL in the range -120 °C and 80 °C, whilst preserving linear dose rate dependence at each irradiation temperature. However, the temperature effect on the RIL signal is still compensable via calibration and temperature monitoring.**

***Index Terms*— Optical Fibers, Dosimetry, Accelerators, Space applications, Radiations, X-rays, Gamma, Silica Glass, Cerium, Copper**

I. Introduction

Radiations are present in various environments around us, originated from natural or man-made sources. On one side, they can be a threat to human health, and also endanger the proper functioning of modern technologies such as optical fibers (OFs). On the other side, there are a large range of clinical applications exploiting the ionizing radiations for either diagnostics or therapeutic uses [1]. The main effect observed on OFs is the Radiation Induced Attenuation (RIA) [2], which increases with the Total Ionizing Dose (TID). RIA amplitude and kinetics depend on many parameters relating to the fiber itself and to its environment [2]. Another observable radiation effect on OFs is the Radiation Induced Emission (RIE) [2]. This RIE occurs when ionizing radiation passes through an optical material and generates photons through Cerenkov effect or through the excitation/emission of point defects and/or active doping centers.

Several ways exist to exploit the luminescence properties of point defects and active centers in the silica fiber materials [3], allowing monitoring environmental parameters such as the dose (fluence) or the dose rate (flux) of particles [4].

Three main types of luminescence processes are often reported:

- Radiation Induced Luminescence (RIL): the emission happens under the irradiation and for some materials, its intensity can be proportional to the particle flux (dose rate).
- Optically Stimulated Luminescence (OSL): in this case, the emission results from recombination processes triggered after the irradiation by a suitable light source. The integrated OSL signal is, for some materials, proportional to the fluence (dose).
- Thermo-Luminescence (TL): similarly to the OSL, an external energy source (heat in this case) induces recombination and consequently light emission after the irradiation. Here again, the integrated TL signal is, for some materials, proportional to the fluence (dose).

Although RIA and RIE are generally a limitation for some applications in harsh environment [5], they are also useful tools to develop radiation monitors and, for the more interesting materials, dosimeters. This study will focus more specifically on the RIL and its potential use for dosimetry in environments combining radiations with temperature variations.

While investigating a fiber-based dosimeter, one can sometimes use commercial OFs exhibiting interesting behavior under irradiation and attempt a calibration in an environment of interest. Nevertheless, in some specific applications, there is a need for dedicated and optimized OFs to reach the expected detection capabilities.

For such purpose, the PhLAM laboratory (Lille, France) developed several silica-based glass rods, with lengths of about 1 cm and diameters from 0.5 to 1 mm, doped with different ions.

Submitted on 11th, November 2020.

N. Kerboub, D. Di Francesca, Y. Kadi, D. Ricci, R. Garcia Alia, M. Brugger are with CERN, 1211 Genève,Suisse.

N. Kerboub, D. Di Francesca, S. Girard, A. Morana, Y. Ouerdane, A. Boukenter, E. Marin are with Univ. Lyon, Laboratoire Hubert Curien - 18 avenue du professeur Lauras, 42000 Saint-Etienne, France

N. Kerboub, J. Mekki are with CNES - 18 Avenue Edouard Belin, 31400 Toulouse, France

H. El Hamzaoui, G. Bouwmans, B. Capoen, R. Habert, M. Bouazaoui, are with Univ-Lille, CNRS, UMR8523 - PhLAM – Physique des Lasers, Atomes et Molécules, CERLA/IRCICA, F-59000 Lille, France

The first was doped with Cu [6]; the second was doped with Ce [7]; and the latter was co-doped with both Cu and Ce [8]. These three samples are referred as Cu, Ce, and CuCe doped rods in the rest of the study. Several studies already demonstrate a promising detection efficiency of these sensors under irradiation at room temperature. These sensors show a linear RIL response versus the dose rate over several decades. The Cu and Ce samples, for instance, have shown linear RIL response up to 30 Gy(SiO_2)/s [6], [7], whereas the CuCe-doped sample exhibited linear RIL response at least up to 34 Gy(SiO_2)/s [8]. In the work presented in [9], the authors showed that the OSL response was linear up to 200 Gy(SiO_2). Furthermore, the Ce and Cu samples were also tested at the TRIUMF facility (Vancouver, Canada) under protons and proved that their RIL response allows monitoring the proton beam flux in the few ms time resolution and that the TID estimation was possible via an integration of the signal over the whole irradiation run [4]. Another advantage of these rods, is that they can be drawn into OFs while keeping their interesting properties to design miniaturized sensors [10], [11].

The performances of such sensors are of interest in the accelerator sector, because they enable the monitoring of some particles beams and secondary showers with time-dependent intensity, such as the accelerators implemented in the CERN accelerator complex [12]. Furthermore, another interesting use at CERN would be the monitoring of the radiation levels in the experiments and shielded areas presented in [13].

Moreover, the space industry is interested as well in such sensors since they allow very efficient radiation detection, opening the way to the monitoring of the low dose rate and flux of particles received by satellites. In the space domain, it is an important task to be able to apply countermeasures on satellites and inhabited missions, in case for instance of solar eruptions [14] endangering electronics systems [15], [16] and humans life.

These application sectors have different constraints but have in common the need of a versatile monitoring system, as resilient as possible against temperature variations during the exposure. For this purpose, this work targets the examination of the RIL of these rods versus temperature.

II. Sensors and Setup Description

A. Silica glass sensors

The samples tested in this work were fabricated by the PhLAM laboratory (FiberTech Lille platform) using the sol-gel technique. At first, cylindrical porous silica monoliths were synthesized starting from tetraethylorthosilicate (TEOS) as precursor. As described in [6], [7], the obtained xerogels were then soaked into Cu, Ce, or Cu and Ce salts-based solution. This process was used to produce the three samples under test, respectively the Cu, Ce and CuCe doped rods. Along with other fabrication processes described in [7], the doped-monoliths were dried to remove the solvent before densification at 1200 °C under helium atmosphere. The densification was performed under inert atmosphere to increase the Cu^+ and Ce^{3+} ions concentration, thus enhancing the RIL efficiency [17]. Finally, the doped glassy rods were drawn at a temperature of about 2000°C down to canes of diameters close to 500 µm. A small portion of each cane (length of about 1 cm) was fusion-spliced, at one end, to a 500-µm diameter pure-silica OF with low index polymer cladding, used as transport fiber in the study. The other end of the transport fiber was connected in front of the detector, PhotoMultiplicator Tube (PMT) or spectrometer.

In the Ce doped sample, the cerium ions are present as Ce^{3+} and Ce^{4+} and the dominant band of the luminescence is attributed to the 5d → 4f transition of Ce^{3+} ions [7]. In the case of the Cu doped sample, the luminescence is mostly associated to the $3d^9 4s \rightarrow 3d^{10}$ ground state level of Cu^+ ions. [6], [9], [10]. The concentration of Copper and Cerium ions were determined using Electron Probe Micro Analysis, and are estimated to 250 and 300 ppm respectively [7], [8], [17]. The concentration of both Cerium and Copper ions in the CuCe co-doped sample are expected to be similar since the same procedure is carried out to perform the doping on either single or co-doped samples.

B. RIL setup, X-ray source and temperature control description

The MOPERIX machine (Laboratoire Hubert Curien, Saint-Etienne, France) offers an irradiation surface of roughly 10×10 cm^2 with 10% dose rate non-uniformity. An X-ray tube placed in the upper part of the irradiation box irradiates the Devices Under Test (DUT) placed below. The tube is operated in this study at 100 kV, providing X-rays with 40 keV energy in average. The operator modulates the dose rate by adjusting the tube supply current, in the range between 0.5 and 45 mA and/or by varying the distance of the DUT with respect to the tube. The reachable dose rate range in the facility is in between 140 µGy(SiO_2)/s and 60 Gy /s, the dose rate is measured with a N23344 soft X-ray chamber as Gy(H_2O). These Gy(H_2O) are converted in Gy(SiO_2) using the NIST database [18] in the range 0.02-0.1 MeV, which is the energy range of the MOPERIX X-rays. In the rest of the paper, all reported dose-rates are in SiO_2. To investigate temperature effects during irradiation, DUTs were set on a thermal plate inside the irradiation box. The temperature of this plate was varied from –120°C to 80°C thanks to external system that controls a resistor plate as well as a pump connected to a liquid nitrogen tank.

Outside the irradiation box, an acquisition system based on a PhotoMultiplier Tube, PMT, (Model H9305-03, Hamamatsu) and a digital scope from Tektronix is used to read and acquire

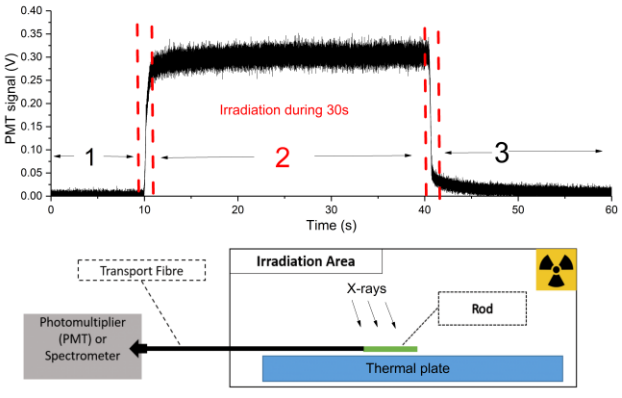

Fig. 1. (a) An example of a typical RIL measurement showing area 1 before irradiation, area 2 during irradiation at constant dose rate, and area 3 after irradiation. (b) Schematics of the experimental setup of the MOPERIX facility, and related acquisition equipment.

the PMT output signal. For some measurements of the study, we replaced the PMT with a mini-spectrometer operating in the UV-visible range, from either Ocean Optics (QE65000) or Hamamatsu (C10083MD). In parallel, a thermocouple on top of the thermal plate provides an online monitoring and recording of the temperature.

III. Experimental Method and Results

A. *Temperature dependence at fixed dose rate*

After placing the sample on the temperature-controlled plate and connecting the transport fiber to the PMT (always set at the same sensitivity), we started an irradiation at room temperature (RT, around 21 °C) and acquired the RIL signal on the oscilloscope. Each irradiation is 30 s long at a fixed dose rate of 184 mGy/s, leading to a TID of 5.5 Gy(SiO_2) per measurement. As shown in Fig.1, the RIL signal quickly increases toward a plateau during the irradiation. The absolute voltage difference between area 1 (PMT noise) and area 2 (PMT noise + RIL signal) of Fig.1, respectively before and during the irradiation, depends on the dose rate. As shown in previous studies [4], [9], [19], the relation between this voltage variation (RIL amplitude) and the dose rate is linear over several decades.

We performed the same operation varying the temperature from RT to -120 °C, acquiring at each temperature step the RIL signal with the same irradiation profile. For each temperature step, we waited ~10 min to ensure the stabilization of the samples temperature before the radiation run. Then, after reaching the lowest temperature, we carried out the same sequence in a reverse order (i.e. from -120 °C to RT). These data are plotted in Fig.2.

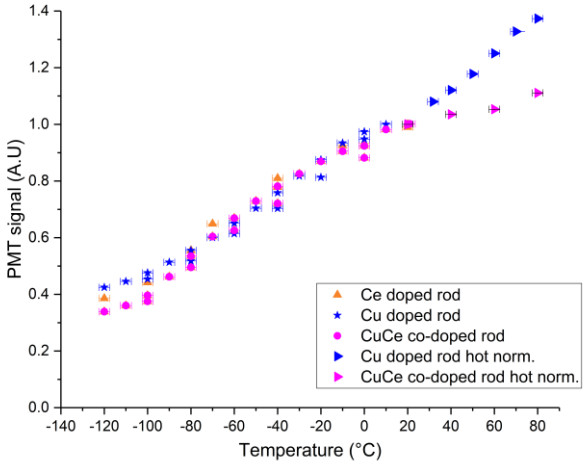

Fig. 2. Rods response measured by the PMT under fixed dose rate (184 mGy/s) for temperature ranging from 20 °C to -120 °C (down-oriented triangular dots) and from -120°C to 20°C (up-oriented triangular dots). Right oriented triangular dots show the normalized measurements from 20°C to 80°C. Error bars on the signal (y-axis) are compatible with the size of the dots.

Because of a technical issue with the plate resistor, we were obliged to replace it with another thermal plate embedding a functioning resistor (for sample heating only), on which we had to move the sample when looking at temperatures higher than RT. This is an important point to keep in mind when analyzing the Fig.2, where the data for the range (-120 °C to RT) are plotted along with a second set of data normalized with the first one at 21°C, from RT to 80 °C (using the heating plate).

Moreover, temperatures above 80 °C were not investigated since this temperature corresponds to the maximum temperature tolerable by the transport fiber coating (~85 °C). In addition, measurements with temperatures above RT were carried out on the Ce- and CuCe-doped samples, whereas unfortunately, it was not possible to perform it on the Cu sample. These sets of experiments will have to be completed in the future.

B. *RIL temperature and dose rate dependence*

The objective in this part was to measure the influence of the temperature on the linearity of the RIL response of the samples.

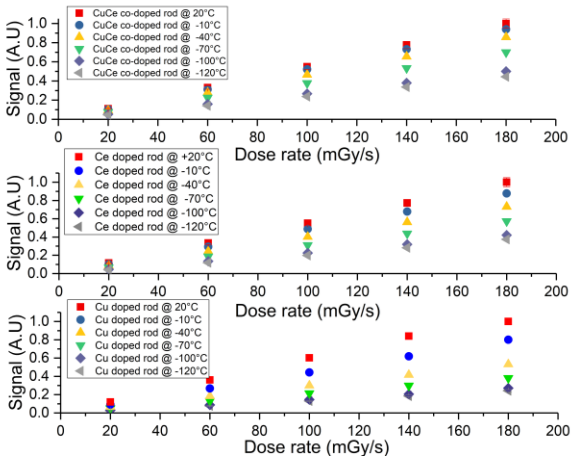

Fig. 3. Rods response measured by the PMT when varying the dose rate from 20 to 184 mGy/s at temperatures ranging from -120 °C to +20 °C. Error bars on the signal (y-axis) are smaller than the dots size.

The dose rate was changed by reducing the current of the tube from 45 mA (corresponding to 184 mGy/s at the test position) to 5 mA (corresponding to 20 mGy/s at the test position). At each step, we have performed a measurement of the response of each sample. Obtained results are illustrated in Fig.3, showing that the linear dose rate dependence of RIL is maintained across the whole tested temperature range.

C. *Spectral RIL temperature dependence*

After the series of measurement carried out with a PMT detection, we changed for a spectrometer to observe the temperature effect on the spectral emission. Using the same thermal plate, we have exposed our samples to temperatures ranging from 20°C to -120°C or (as in a Fig. 6) from 0°C to -120ºC because of a lack of time. We kept the same fixed dose rate as earlier in this study (184 mGy/s).

The first tested sample is the Ce-doped rod, which exhibits a band maximum around 470 nm, as shown in Fig. 4, the second is the Cu-doped rod, which emits light around 550 nm, whereas the CuCe doped rod resembles a combination of the two previous spectra.

In the top plots of Fig.4 to Fig.6, we plotted the spectrum acquired at different temperatures, after normalization to the maximum peak amplitude, which allows focusing on the shape of the spectrum. We observe that the three samples keep a very similar spectral band shape over the investigated temperature range.

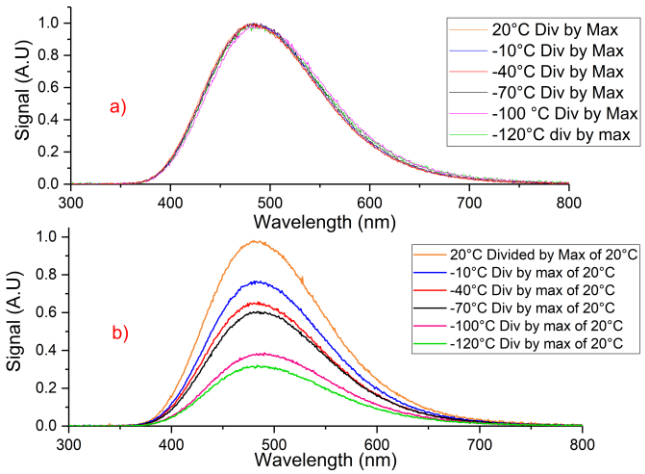

Fig. 4. Cerium-doped rod spectral RIL response for temperature ranging from 20°C to -120°C. a) Top – Each curve is normalized to its maximum peak value b) Bottom – Each curve is normalized to the maximum peak value at 20°C.

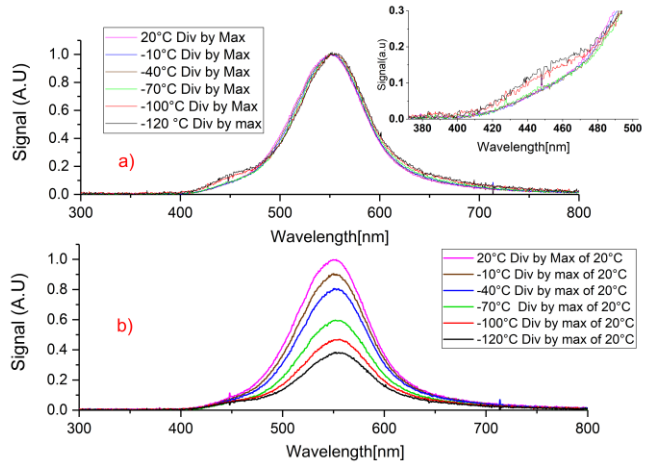

Fig. 5. Copper doped rod spectral RIL response for temperature ranging from 20°C to -120°C. a) Top – Each curve is normalized to its maximum peak value b) Bottom – Each curve is normalized to the maximum peak value at 20°C.

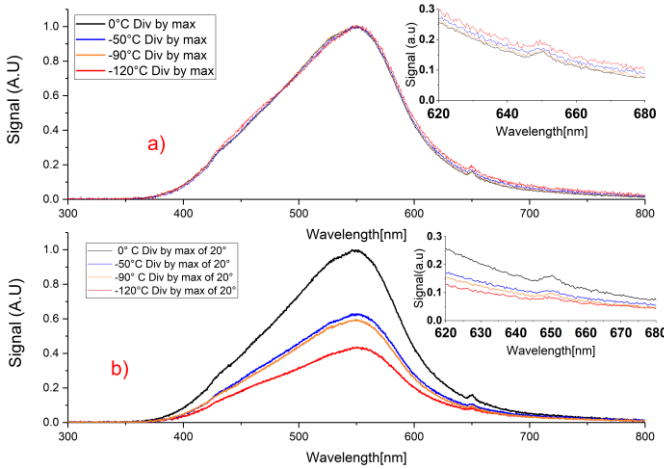

Fig. 6. CuCe co-doped rod spectral RIL response for temperature ranging from 0°C to -120°C. a) Top – Each curve is normalized to its maximum peak value. b) Bottom – Each curve is normalized to the maximum peak value at 20°C.

Secondly, on the bottom plots of the Fig.4 to Fig.6 we plotted the spectrum acquired at different temperatures, normalized to the maximum peak amplitude measured at 20°C, which permits focusing on amplitude variations versus temperature. At first sight, we notice that the signal amplitude decreases when lowering the temperature, which is compatible with the observations made during the PMT acquisition (Fig.2).

D. Estimation of the respective contributions of Cu and Ce dopants to the emission of CuCe doped rod

After investigating the RIL response of both Cu and Ce doped rods, we know their respective emission spectrum that are plotted in Fig.5 and Fig.6. Similarly, we have the RIL emission spectrum of the CuCe co-doped rod plotted in Fig.6.

Owing to the fact the samples are manufactured following the same process, using the same dopants, we would like to investigate if the spectral shape of the CuCe doped sample can be reproduced by a linear combination of the Cu and Ce doped samples spectra. To this end, we carried out on the normalized CuCe co-doped sample spectrum a linear regression on the CuCe sample spectrum using the normalized Cu and Ce emission spectra as base components.

Finally, we plotted in Fig.7 the CuCe co-doped rod emission along with that obtained with the linear combination of Cu and Ce doped rod emissions. The best linear combination found is $(0.445\pm0.0015)*Ce_{emission} + (0.752\pm0.0018)*Cu_{emission}$ with $Cu_{emission}$ and $Ce_{emission}$ the respective RIL emission spectrum of Cu- and Ce-doped rod. As a result, we observe that the obtained spectrum plotted as "FIT (Cu + Ce)" in Fig. 7, is in good agreement with the CuCe co-doped rod spectra plotted in the same figure. The absolute difference between both emission spectra is also plotted.

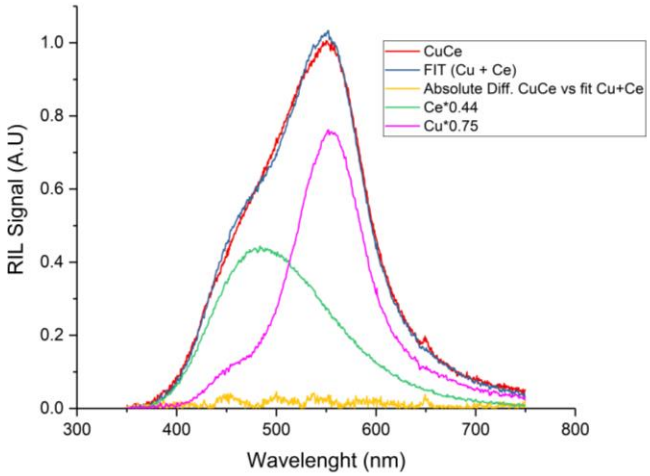

Fig. 7. Spectral RIL response of the CuCe co-doped rod, and a linear regression estimating the respective contribution of the Cu and Ce compounds to the CuCe-doped rod RIL. Both Cu and Ce responses multiplied by respective coefficients, and difference between the linear fitting versus CuCe response are also shown.

IV. Discussion

The results of the experiment exhibit interesting and similar trends for the three samples. First, as shown in Fig.2, we observe a lowering of the signal amplitude with the reduction of the temperature. The slopes of the curves are very similar for all the tested samples and show a loss of roughly 60 % of the signal at -120 °C with respect to that measured at 20 °C. This temperature dependence may be explained by the fact that the RIL phenomenon is somehow assisted by phonons. At the same time, increasing temperature normally leads to enhanced non-radiative de-excitation of the emitting centers, and a consequent weakening of the associated emission. Therefore, our results might show that phonons play an important role in the excitation process of the emitters. This preliminary hypothesis will be subject to further investigation.

In addition, the measurement points from 20°C to -120°C overlaps with those obtained from -120°C to 20°C, which means that the response is completely reversible. Such a temperature dependence of the RIL is easily compensable with an appropriate calibration, provided that the temperature is measured simultaneously with the RIL signal. Indeed, a pre-calibration of the sensors and a post-processing would permit extracting precise dose rate measurements.

We did not observe any effect on the linearity of RIL *vs* dose rate for all the tested samples. As shown in Fig. 3, for the three samples, the signal remains linear versus the dose rate at least over one order of magnitude, for temperatures ranging from -120 °C to RT. In addition, spectral measurement of the RIL emission acquired on the samples shows that the spectral shape remains similar over the range of temperature investigated during this experiment, except for one band. By contrast, the temperature affects the amplitude of the emission band, accordingly to what we observed with the PMT measurements in Fig. 2. As shown in Fig. 5, in the Cu-doped rod response, we can observe a change around 440 nm, where the relative amplitude seems to increase while lowering the temperature. This emerging band can be attributed to the emission from Cu^+ ions in eight-coordinated cubic sites, that might exist in silica glass, as reported by Debnath and Das [20]. The corresponding transitions would be less affected by the phonon-mediated processes. .

Besides, we have a weak and narrow peak around 650 nm (see insets in Fig. 6). This band is only observable in the CuCe co-doped rod response, and have not been reported in another study on CuCe co-doped samples [8]. We are not able so far to identify the potential origin of this band, although we tend to exclude a parasitic origin that would be otherwise present also in the spectra of the other samples.

At last, we have estimated the respective contribution of Cu and Ce dopants, to the CuCe co-doped rod RIL emission. The difference between the linear combination and the CuCe spectrum could potentially be attributed to the variability of the measurement conditions and potentially to material production. Particularly, the dopant environment may be not exactly the same between the single-doped samples and the co-doped one. However, this difference is sufficiently small to conclude that the Cu and Ce dopants does not interact significantly in the CuCe co-doped silica glass and that the color centers related to Cu^+ and Ce^{3+} are essentially the same ones than in the samples doped with a sole ion type.

V. Conclusion and outlook

In this study, we have performed measurements on Cu, Ce and CuCe co-doped silica glass rods fabricated by FiberTech Lille (PhLAM laboratory). These rods showed very interesting detection capabilities of X-ray and protons, thanks to the linear response of the RIL signal over several order of magnitudes in dose rate. An important additional step was to provide information about the temperature effect on the RIL signal. For this purpose, we have carried out a study on the samples under X-rays at Laboratoire Hubert Curien, for temperatures ranging from -120 °C to RT and in a second time, from 20 °C to 80 °C. We observed a dependence of the RIL signal level over temperature for the three samples, but this dependence is still compensable via calibration and temperature monitoring. Despite changing temperature has an effect on the signal amplitude, the linear response of the sensors at each temperature is preserved. Therefore, these sensors could potentially trigger the interest of the industry/research sector, for dosimetry in harsh environment.

In the future, we plan to investigate more in the details the thermal dependence of the samples emission in order to identify the mechanisms behind it, so as we could in the future, reduce or compensate such effects.

.

VI. References

[1] *Radiation in Medicine: A Need for Regulatory Reform*. Washington, D.C.: National Academies Press, 1996, p. 5154.

[2] S. Girard *et al.*, “Radiation Effects on Silica-Based Optical Fibers: Recent Advances and Future Challenges,” *IEEE Trans. Nucl. Sci.*, vol. 60, no. 3, pp. 2015–2036, Jun. 2013, doi: 10.1109/TNS.2012.2235464.

[3] G. Pacchioni, L. Skuja, and D. L. Griscom, Eds., *Defects in SiO2 and Related Dielectrics: Science and Technology*. Dordrecht: Springer Netherlands, 2000.

[4] S. Girard *et al.*, “Potential of Copper- and Cerium-Doped Optical Fiber Materials for Proton Beam Monitoring,” *IEEE Trans. Nucl. Sci.*, vol. 64, no. 1, pp. 567–573, Jan. 2017, doi: 10.1109/TNS.2016.2606622.

[5] S. Girard *et al.*, “Integration of optical fibers in radiative environments: Advantages and limitations,” in *2011 2nd International Conference on Advancements in Nuclear Instrumentation, Measurement Methods and their Applications*, Ghent, Belgium, Jun. 2011, pp. 1–6, doi: 10.1109/ANIMMA.2011.6172874.

[6] B. Capoen *et al.*, “Sol–gel derived copper-doped silica glass as a sensitive material for X-ray beam dosimetry,” *Opt. Mater.*, vol. 51, pp. 104–109, Jan. 2016, doi: 10.1016/j.optmat.2015.11.034.

[7] H. El Hamzaoui *et al.*, “Cerium-activated sol–gel silica glasses for radiation dosimetry in harsh environment,” *Mater. Res. Express*, vol. 3, no. 4, p. 046201, Apr. 2016, doi: 10.1088/2053-1591/3/4/046201.

[8] J. Bahout *et al.*, “Cu/Ce-co-Doped Silica Glass as Radioluminescent Material for Ionizing Radiation Dosimetry,” *Materials*, vol. 13, no. 11, p. 2611, Jun. 2020, doi: 10.3390/ma13112611.

[9] N. Al Helou *et al.*, “Optical responses of a copper-activated sol-gel silica glass under low-dose and low-dose rate X-ray

exposures," *OSA Contin.*, vol. 2, no. 3, p. 563, Mar. 2019, doi: 10.1364/OSAC.2.000563.
[10] H. El Hamzaoui *et al.*, "Sol-gel derived ionic copper-doped microstructured optical fiber: a potential selective ultraviolet radiation dosimeter," *Opt. Express*, vol. 20, no. 28, p. 29751, Dec. 2012, doi: 10.1364/OE.20.029751.
[11] J. Bahout *et al.*, "Remote Measurements of X-rays Dose Rate using a Cerium-doped Air-clad Optical Fiber," *IEEE Trans. Nucl. Sci.*, pp. 1–1, 2020, doi: 10.1109/TNS.2020.2972043.
[12] L. Evans and P. Bryant, "LHC Machine," *J. Instrum.*, vol. 3, no. 08, pp. S08001–S08001, Aug. 2008, doi: 10.1088/1748-0221/3/08/S08001.
[13] R. Garcia Alia *et al.*, "LHC and HL-LHC: Present and Future Radiation Environment in the High-Luminosity Collision Points and RHA Implications," *IEEE Trans. Nucl. Sci.*, vol. 65, no. 1, pp. 448–456, Jan. 2018, doi: 10.1109/TNS.2017.2776107.
[14] Sé. Bourdarie and M. Xapsos, "The Near-Earth Space Radiation Environment," *IEEE Trans. Nucl. Sci.*, vol. 55, no. 4, pp. 1810–1832, Aug. 2008, doi: 10.1109/TNS.2008.2001409.
[15] D. Binder, E. C. Smith, and A. B. Holman, "Satellite Anomalies from Galactic Cosmic Rays," *IEEE Trans. Nucl. Sci.*, vol. 22, no. 6, pp. 2675–2680, 1975, doi: 10.1109/TNS.1975.4328188.
[16] D. M. Fleetwood, P. S. Winokur, and P. E. Dodd, "An overview of radiation effects on electronics in the space telecommunications environment," *Microelectron. Reliab.*, vol. 40, no. 1, pp. 17–26, Jan. 2000, doi: 10.1016/S0026-2714(99)00225-5.
[17] H. E. Hamzaoui *et al.*, "Effects of densification atmosphere on optical properties of ionic copper-activated sol–gel silica glass: towards an efficient radiation dosimeter," *Mater. Res. Express*, vol. 1, no. 2, p. 026203, Jun. 2014, doi: 10.1088/2053-1591/1/2/026203.
[18] "NIST X-Ray Mass Attenuation Coefficients," *NIST X-Ray Mass Attenuation Coefficients*. https://physics.nist.gov/PhysRefData/XrayMassCoef/tab3.html.
[19] N. Al Helou *et al.*, "Radioluminescence and Optically Stimulated Luminescence Responses of a Cerium-Doped Sol-Gel Silica Glass Under X-Ray Beam Irradiation," *IEEE Trans. Nucl. Sci.*, vol. 65, no. 8, pp. 1591–1597, Aug. 2018, doi: 10.1109/TNS.2017.2787039.
[20] R. Debnath and S. K. Das, "Site-dependent luminescence of Cu+ ions in silica glass," *Chem. Phys. Lett.*, vol. 155, no. 1, pp. 52–58, Feb. 1989, doi: 10.1016/S0009-2614(89)87359-2.